Journal of Physics: Conference Series **438** (2013) 012017 doi:10.1088/1742-6596/438/1/012017

Channeling and Radiation of Electrons in Silicon Single Crystals and $Si_{1-x}Ge_x$ Crystalline Undulators

H Backe[1], D Krambrich[1], W Lauth[1], K K Andersen[2], J Lundsgaard Hansen[2] and and Ulrik I Uggerhøj[2]

[1] Johannes Gutenberg-University Mainz, Institute for Nuclear Physics, D-55099 Mainz, Germany

[2] University of Aarhus, Department of Physics and Astronomy, DK-8000 Aarhus C, Denmark

E-mail: backe@kph.uni-mainz.de

Abstract. The phenomenon of channeling and the basic features of channeling radiation emission are introduced in a pedestrian way. Both, radiation spectra as well as dechanneling length measurements at electron beam energies between 195 and 855 MeV feature quantum state phenomena for the (110) planar potential of the silicon single crystals. Radiation from a crystalline undulator, produced at the Aarhus University (UAAR), has been investigated at the Mainz Microtron electron accelerator facility MAMI. The 4-period epitaxially grown strained layer $Si_{1-x}Ge_x$ undulator had a period length λ_u= 9.9 μm. At a beam energy of 375 MeV a broad excess yield around the theoretically expected photon energy of 0.132 MeV has been observed. Model calculations on the basis of synchrotron-like radiation emission suggest that evidence for a weak undulator effect has been observed.

1. Introduction

In order to understand the phenomenon of planar channeling, it suffices to envisage a single crystal as composed of planes (sheets) in the average potential of wich the transverse motion of a particle can be bound. This way the particle can be steered over long longitudinal distances. The situation is quite similar as for people walking between grape-vines, see Fig. 1.[1] In this article we focus on channeling of electrons. Electrons have, in contrast to positrons, a much greater chance to interact with positively charged atomic nuclei comprising a plane. Consequently they have a much shorter dechanneling length. The latter characterizes the mean distance a particle is bound in the potential well. Imagine in Fig. 1 a violent interaction of a person with a grape-vine tree. It probably will finish the walk.

In general the particle oscillates in the potential well as shown in Fig. 2, right panel, and thereby so called channeling radiation is emitted. Although the potential depths are in the laboratory frame for positrons or electrons only in the order of some tens of eV, the oscillation may result in photons with energies in the range between keV to multi MeV if the relativistic particle energies are in the range between a few MeV to some GeV, respectively. How this feature comes about is explained in section 2.1 of this paper.

[1] For the Romans Mogontiacum, first mentioned by Tacitus (about 58-120 AD), now Mainz, was a military base to protect the empire against barbarians living in the north of the river Rhine. Vine was an important beverage for the troops. To avoid the cumbersome transport of vine in amphoraes over the Alps, Romans started in the third century to cultivate vine-growing also in the region around Mainz.

Figure 1. Left: A colorful way to demonstrate channeling. Picture captured by one of us (H.B.) at the vineyard Baiken at Rauenthal, Rheingau, Germany. Right: Channeling of a positively charged particle. Shown are two strings of atoms composing crystal planes.

If the crystal planes are periodically bent at the direction the particle moves, undulator-like radiation in the hundreds of keV up to the MeV region may be emitted in addition to channeling radiation. The possibility to produce very intensive γ-ray sources in the MeV range at channeling of electrons or positrons has been discussed theoretically since the mid 70th of the last century [1, 2, 3]. Nowadays this field of research has been matured and detailed theoretical predictions on the feasibility of a γ-ray laser on the basis of micro undulators have been made, for an overview see Ref. [4], and the recent text book of A. V. Korol, A. V. Solov'yov, and W. Greiner [5], and references cited therein. However, the experimental demonstration of such devices hampers essentially from two obstacles. On the one hand, high quality positron beams in the GeV range are not easily available, in contrast to electron beams, and, on the other hand, crystal-undulator production and characterization of their features are still in a rather rudimentary stage. Because of this situation, experiments have been commenced at the Mainz Microtron MAMI, where a high quality electron beam with energies of up to 855 MeV is available. The aim is to characterize epitaxially produced $Si_{1-x}Ge_x$ superlattices [6, 7] [2] designed as crystal undulators. Periodically undulating (110) planes can be obtained by a variation of the concentration x, for details see e.g. Ref. [9, 11].

Preliminary experimental results with a 4-period undulator with period length of 9.9 μm, grown at the Aarhus University, have been described in recent papers [10, 11]. Clear enhancements of intensities were observed in the energy region where the undulator radiation peak is expected. However, only weak evidence for a small peak was observed at the beam energy of 270 MeV [11]. Simulation calculations of the undulator radiation spectra have been performed on the basis of synchrotron-like radiation emission which suggest a very small coherence effect. To figure out the reason for the obviously very small dechanneling length, we focus in this contribution on the analysis of another measurement with the same undulator at a somewhat higher beam energy of 375 MeV. Experiment and model calculations are described in sections 3 and 4. In addition, we reanalyzed dechanneling length measurements already published in Ref. [12] under refined model assumptions. The results are presented in subsection 2.3.

For readers only interested to understand principles, a pedestrian introduction to the phenomenon of channeling radiation emission is presented in subsections 2.1 and 2.2.

[2] For earlier references on the structure, properties and applications of $Si_{1-x}Ge_x$ strained layers and superlattices see the review article Ref. [8].

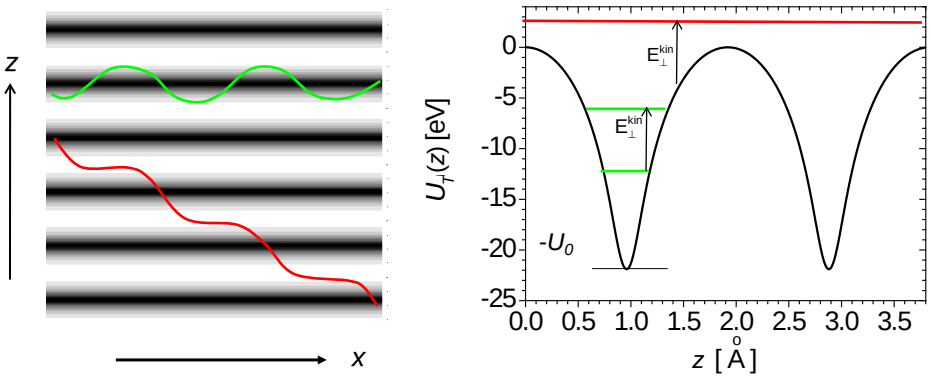

Figure 2. Left: Density plot of the mean potential of planes in a single crystal. White corresponds to a low and black to high potential for a positive probe charge. The transverse motion of an electron in a bound state is called planar channeling, and in an unbound state of low continuum energy planar quasi-channeling. Right: Cut through the potential along the z axis. The energy is given by the potential at the point of impact to which the transverse kinetic energy $E_\perp^{kin} \approx pv \cdot \psi_\perp^2/2$ must be added, with $\psi_\perp$ the tilt angle of the impinging electron with respect to the (110) planes and pv the momentum of the particle. For further details see also Ref. [22].

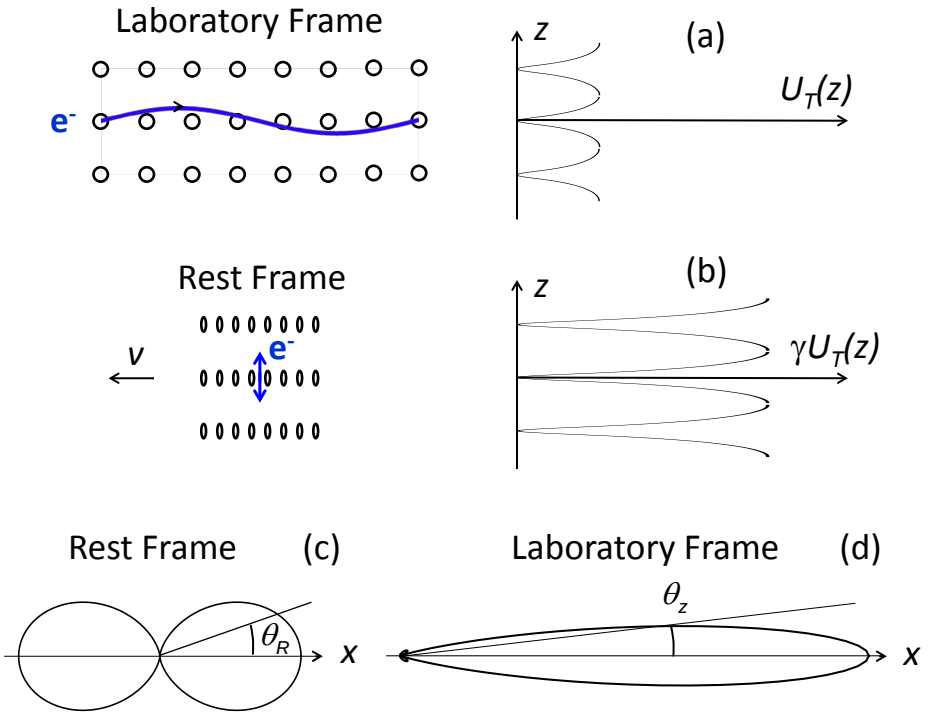

Figure 3. Explaining the basic features of channeling radiation. Shown are the potential for an electron at (110) planar channeling in a silicon single crystal in the laboratory frame (a), and in the rest frame of the electron (b), angular distribution of the emitted radiation in the dipole approximation in the rest frame (c), and in the laboratory frame (d). In this example the Lorentz factor is $\gamma = 3$.

2. Channeling and channeling radiation

The phenomena of channeling and channeling radiation emission have been studied by a number of authors, both theoretically as well as experimentally. In the following only the most important facts are compiled for the purpose that an interested non-specialized reader may be able to qualitatively understand the subject of this article. Comprehensive overview articles have been written to which advanced readers in this field of research are referred to [13, 14, 15, 16, 17, 18, 19, 20, 21].

2.1. Basic features of channeling radiation emission

Let us first understand how the high photon energies observed in the laboratory system come about. As shown in Fig. 3 (a) and (b) the electron sees in its rest frame a Lorentz contracted lattice. This fact results in an increase of the potential depth by the Lorentz factor $\gamma = (1-\beta^2)^{-1/2}$, with $\beta = v/c$ the reduced velocity of the electron in the laboratory system, and, accordingly, also of the emitted photon energy. The emission characteristics for a dipole transition $dn_R/d\Omega_R \propto \cos^2\theta_R$ in the rest frame of the electron is depicted in Fig. 3 (c). Note that the angle θ_R is the angle between the x axis and the emission direction, and not between the dipole moment and the emission direction. The angular distribution in the laboratory frame, given by the equation [23]

$$\frac{dn}{d\Omega} = \frac{dn_R}{d\Omega_R}\frac{d\Omega_R}{d\Omega} = \frac{dn_R}{d\Omega_R}\frac{1}{\gamma^2(1-\beta\cdot\cos\theta)^2}, \tag{1}$$

is strongly forward directed, see Fig. 3 (d).

So far channeling has been treated as a pure classical phenomenon. However, in reality quantum states exist in the potential well and a transition may result in emission of monochromatic radiation. Deexcitation photons emitted in the rest frame of the electron are boosted in the laboratory system to an energy [14]

$$\hbar\omega = \frac{\hbar\omega_R}{\gamma(1-\beta\cdot\cos\theta)} \cong \frac{2\gamma^2}{1+(\theta\gamma)^2}\hbar\omega_0. \tag{2}$$

At the right side of this equation $\hbar\omega_R = \gamma\hbar\omega_0$ has been substituted with the transition energy in the potential well in the laboratory frame $\hbar\omega_0$, see Fig. 3 (a).

2.2. Quantum states and channeling radiation

To calculate the energy levels in the potential well, we follow Ref. [19, Eqn. (2.189)]. The potential has been approximated by $U_T(z) = U_0/\cosh^2(z/b)$ with $U_0 = 22.9$ eV, $b = 0.303$ Å for which the one dimensional Schrödinger equation can be solved analytically. The solution for the eigenstates reads

$$\varepsilon_n = -\frac{(\hbar c)^2}{2\gamma m_e c^2 b^2}\left(-\frac{1}{2}+\sqrt{\frac{1}{4}+\frac{2\gamma m_e c^2 U_0 b^2}{(\hbar c)^2}}-n\right)^2, \quad 0 \le n \le -\frac{1}{2}+\sqrt{\frac{1}{4}+\frac{2\gamma m_e c^2 U_0 b^2}{(\hbar c)^2}} \tag{3}$$

with the quantum number n being 0 or a positive integer. As an example, the experimental photon spectra in Fig. 4 are the result of (110) planar channeling of electrons in a silicon single crystal. Shown are also corresponding calculated level schemes. The photon energy for a transition $\varepsilon_i - \varepsilon_f$ between two levels in the potential well is given according to Eqn. (2) by $\hbar\omega \simeq 2\gamma^2(\varepsilon_i - \varepsilon_f)$ at $\theta = 0$. It is interesting to notice that $\varepsilon_i - \varepsilon_f$ scales for low principal quantum numbers about proportional to $\gamma^{-1/2}$ similar as for an harmonic oscillator, see Ref. [14, p. 458 f]. This behavior originates from the fact that the potential at the minimum can well be approximated by a harmonic oscillator potential.

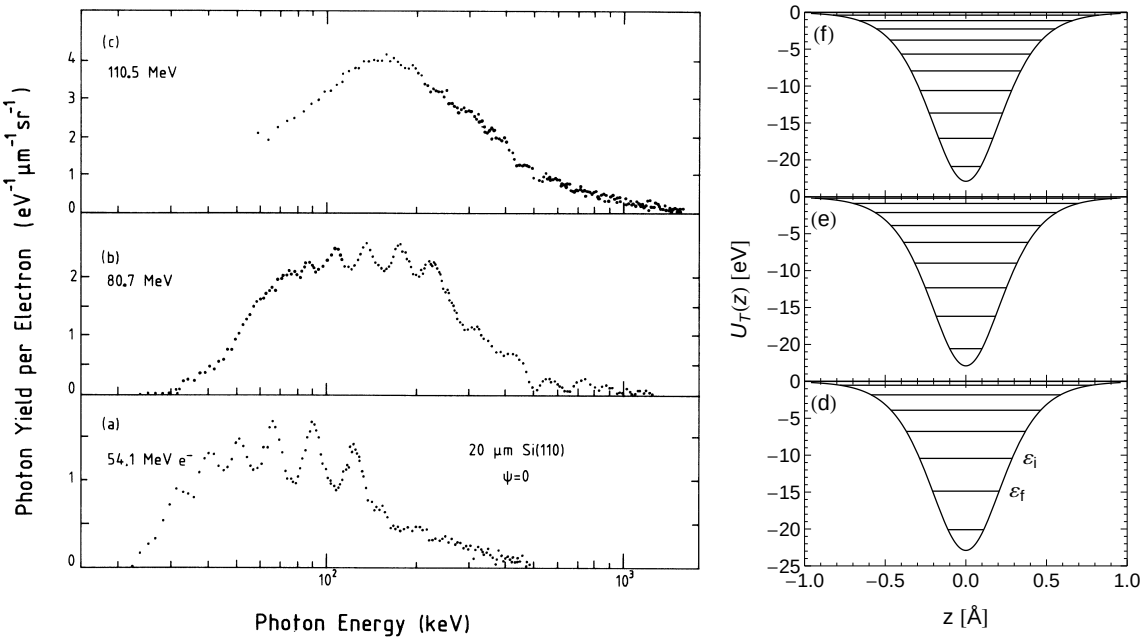

Figure 4. Radiation spectra for 54.1 (a), 80.7 (b), and 110.5 MeV (c) electrons incident along the (110) planar direction of a 20 μm silicon single crystal. Spectra at random orientation of the crystals were subtracted. Figure taken from Ref. [26]. Panels (d), (e), and (f) show corresponding level schemes. The potential is an approximation which allows to solve the one-dimensional Schrödinger equation analytically [19, Eqn. (2.189)].

The line structure disappears at the electron energy of 110.5 MeV for which the level density is so high that the lines overlap. The line width originates mainly from incoherent scattering of the electrons on lattice atoms resulting in the creation or absorption of phonons (also frequently called in literature thermal scattering) [3], as well as from multiple scattering. The latter is effective only for the dimension parallel to a crystallographic plane, since perpendicular to a plane the electron is bound and a scattering process results in a transition between levels in the potential well or into the continuum. Coherence lengths calculations were presented in a number of papers for various transitions and crystals, however, an disentanglement between incoherent scattering, leading to a Lorentzian line shape, and multiple scattering with a Gaussian line shape was first performed in Ref. [27] for diamond single crystals. As for diamond, the coherence length is expected also for silicon to be in the order of a μm decreasing slowly as function of increasing beam energy, see Ref. [27, TABLE I]. Indeed, at a beam energy of 110.5 MeV an assumed coherence length $l_{coh} \simeq 0.5$ μm results for $\varepsilon_1 - \varepsilon_0 = 3.8$ eV in a relative line widths $\Gamma/\hbar\omega = \hbar c/[l_{coh}(\varepsilon_i - \varepsilon_f)] = 10$ % (FWHM). At the corresponding photon energy at observation in forward direction $\hbar\omega = 355$ keV the width amounts to $\Gamma = 37$ keV which can hardly be resolved at a typical energy separation of the photon lines of also 10 %. At still higher electron energies only smooth structures are observed for the same reasoning. However, it is an open question up to which beam energy the lowest bound states cannot be treated classically, meaning that for the dechanneling length additional considerations are required. In trying to answer this question, dechanneling length measurements performed for the relevant beam energies between 195 and 855 MeV at the Mainz Microtron MAMI [12] have been reanalyzed.

[3] We mention that the line broadening effect due to incoherent scattering has some similarity with the well known collisional line broadening in atomic physics.

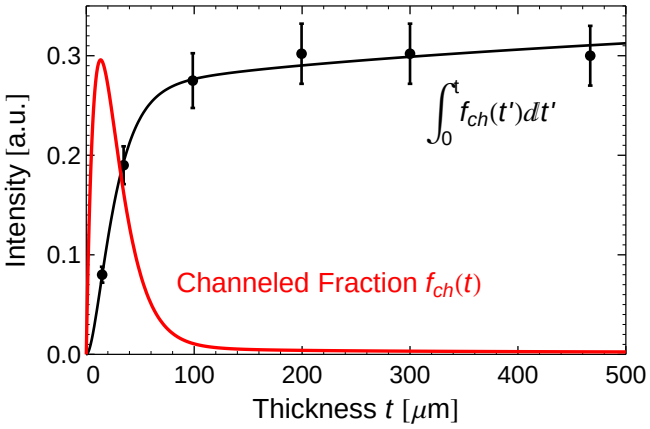

Figure 5. Dechanneling length measurement at a beam energy of 855 MeV. Error bars indicate the experimental signal as function of the crystal thickness. The signal was generated by electrons which have lost about 50 % of their primary energy. For experimental details see Ref. [32]. The red curve assigned with "Channeled Fraction f_{ch}" is the occupation probability according to Eqn. (4) with $a = 0.01$ and $t_0 = 6$ μm. The black curve assigned with $\int_0^t f_{ch}(t')dt'$ is the integrated channeled fraction fitted to the data.

2.3. Dechanneling length in the quantum state picture

One of the very important prerequisites for experimental studies of undulator-like radiation in strained-layer $Si_{1-x}Ge_x$ superlattices is the knowledge of the dechanneling length of electrons for the (110) crystallographic plane. Unfortunately, even for undistorted plane crystals only little is known experimentally. Because of this fact, we have performed dechanneling length measurements at various beam energies for plane crystals. The results were published in Ref. [32]. In Fig. 5 a typical measurement is depicted here once more.

The most striking feature is the approximative signal saturation as function of the crystal thickness t. Such a behavior is not at all expected in the classical picture, based on the Fokker-Planck equation, for the fraction of electrons residing in the potential pocket. A strong rechanneling probability causes a much steeper increase of the total probability as function of increasing crystal thickness, see Ref. [25, Fig. 16]. Therefore, it might be tempting to speculate that the signal originates from the lowest quantum state in the potential pocket. With the probability density maximum at atomic planes a large probability for collisions with small impact parameters may result which probably are required for the large energy loss of the electron of about 50 % of their primary energy. However, there is indication for a small rechanneling probability at larger crystal thicknesses which was neglected in our previous analysis. In the latter it was assumed that the probability density $f_{ch}(t)$ is proportional to $\exp(-t/L_d)$ meaning that the occupation probability has its maximum already at $t = 0$ from where it decays exponentially with the characteristic dechanneling length L_d. This assumption is questionable in the quantum picture since the lowest quantum state might also be occupied by radiative transitions.

This discussion led us for the probability density $f_{ch}(t)$ to a differential equation of the type

$$\frac{df_{ch}(t)}{dt} + \frac{f_{ch}(t)}{L_d} - r_0 \cdot r(t)(1 - f_{ch}(t)) = a \exp\left[-\frac{t}{t_0}\right] \quad (4)$$

$$g_{ch}(t) = C \int_0^t f_{ch}(t')dt' \quad (5)$$

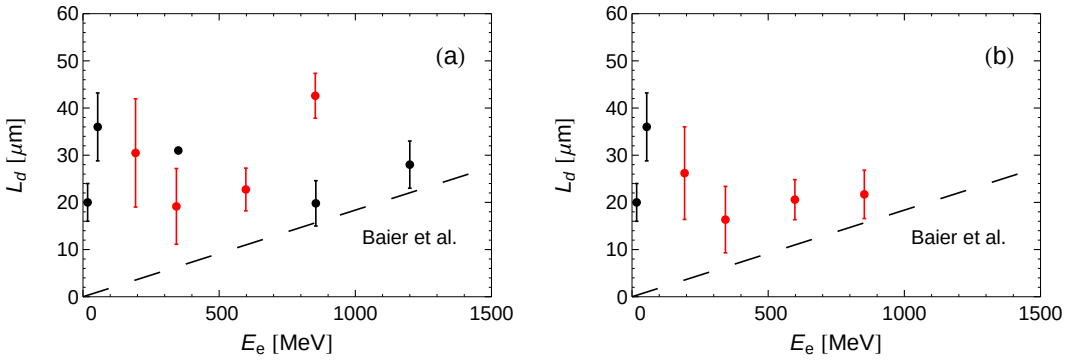

Figure 6. Dechanneling lengths for (110)-planar channeling of electrons at silicon single crystals as function of the electron energy. The experimental values assigned in black are for 17 MeV and 54 MeV the 1/e occupation lengths derived from the 1→ 0 radiative transition [28]. The point at 350 MeV is taken from Ref. [29] for which no error bar has been quoted. The value at 855 MeV is a reanalysis of the measurement published in Ref. [25, Fig. 15] with allowance for rechanneling, and the value at 1200 MeV is taken from Ref. [30]. The reanalysis of measurements at MAMI [32] are shown with red error bars for two models: Model (I) assumes prompt feeding taking into account rechanneling (a), model (II) assumes delayed feeding (b). The dashed line assigned with "Baier et al." is a calculation according to Ref. [31, Eqn. (10.1)] with $U_0 = 22$ eV.

which must be solved to obtain the fit function Eqn. (5). The latter is the integral over the crystal thickness t of the solution of Eqn. (4). The solution of the truncated differential equation $df_{ch}/dt + f_{ch}/L_d = 0$ is simply the already mentioned exponential function. The third term on the left hand side of the differential equation (4) takes into account rechanneling. It has been assumed that it is proportional to the occupation probability for an electron in the potential pocket obtained from the solution of the Fokker-Planck equation for 855 MeV electrons [25] for which the function $r(t) = \sqrt{t_s/(t+t_s)}$ with $t_s = 2.68$ μm is a good approximation. The function $\exp[-t/t_0]$ on the right hand side takes into account a possible delayed feeding of the quantum state.

For the best fit procedure two model assumptions have been tested. For model (I) the homogeneous differential equation (4) with $a = 0$ has been solved. The dechanneling length L_d, the rechanneling parameter r_0 and the common overall factor C at the integral for $g_{ch}(t)$ were taken as free fit parameters assuming for the initial occupation $f_{ch}(t \to 0) = 0.5$. This procedure is equivalent to a prompt feeding of the bound level. The fit results are shown in Fig. 6 (a). In model (II) a delayed feeding of the lowest bound state has been assumed by solving the inhomogeneous differential equation with $a \neq 0$ and choosing $f_{ch}(t \to 0) = 0$ as initial occupation, selecting a proper t_0 with the boundary condition of a constant product $a \cdot t_0 = 0.06$, and treating for the best fit procedure again the three above mentioned parameters as free. The results are shown in Fig. 6 (b).

2.4. Discussion of the dechanneling length measurements

From the classical model of Baier et al. [31, Eqn. (10.1)] a linear increase of the dechanneling length as function of the electron energy is expected. However, the experimental data suggest a significant larger dechanneling length for our measurement at 195 MeV in accord with the data points at 17 and 54 MeV taken from Ref. [28]. We interpret this finding is indication for a quantum state effect at dechanneling also for the beam energy of 195 MeV. Comparing the results for the measurements at 195, 345 and 600 MeV depicted in Fig. 6 (a) and (b) we see that the two model assumptions result in more or less the same dechanneling lengths. This is not

surprising since the parameter $t_0 = 1$ μm had to be chosen rather small (with one exception).

A special case are the two measurements at 855 MeV for which model (I) gives quite different results. A significant better fit to the upper red data point was obtained with model (II) by choosing $t_0 = 6$ μm, this example is shown in Fig. 5, resulting in the shown decrease of the dechanneling length in Fig. 6 (b). Indeed, with this choice of the delayed feeding parameter t_0 it does not contradict the reanalyzed measurement from Ref. [25, Fig. 15] with allowance for rechanneling, see black error bar in Fig. 6 (a). However, the analysis procedures are inconsistent since for this black data point we found no indication for a delayed feeding.

In summary of this part, the nearly saturated signals as function of the crystal thickness, see for an example Fig. 5, as well as the reanalysis for the dechanneling lengths both provide evidence for quantum state effects. It manifests itself for the measurement at 195 MeV in a significant larger dechanneling length in comparison with the classical model of Baier et al. [31, Eqn. (10.1)]. For the measurement at 855 MeV we obtained inconsistent results. Obviously, the experimental data basis is not good enough for a definite assignment of the dechanneling length. Much more data points should be taken, in particular at crystal thicknesses less than about 20 μm including measurements with very thin crystals in the order of only a few μm.

Let us finish this subsection with a qualitative discussion how a longer quantum state dechanneling length emerges in comparison with the classical picture. As already mentioned, at the crystal entrance face well separated low lying quantum states may be populated either directly or delayed. In both cases the excitation of an electron from the ground state level requires a single scattering of the electron with a minimum scattering angle $\Delta\psi_\perp^2 \approx 2\Delta E_\perp^{kin}/(pv)$, with $\Delta E_\perp^{kin} \simeq 60$ eV$/\sqrt{\gamma}$ the transverse energy transfer for the transition to the first excited state. For this approximation $\gamma \gtrsim 200$ must be fulfilled. At an electron energy of 855 MeV an angle $\sqrt{\Delta\psi_\perp^2} = 59$ μrad results. To reach the region with high level density, this angle might even be larger by a factor of about 3-4. Such single scattering events might have a low probability even if taken into account that the angular integration extends to infinity and the probability density of the electron at the crystal plane is high. As a result, a longer ″quantum state″ dechanneling length might be the consequence, even at a beam energy as high as 855 MeV, in contrast to a weakly bound classical state. For the low beam energies of 17 and 54 MeV ″quantum state″ effects are well known. The term ″occupation length″ used in Ref. [28] is actually a synonym for our dechanneling length. [4]

3. Experiments with the crystalline undulator at 375 MeV beam energy

In the following we report on an experiment performed with a 4-period $Si_{1-x}Ge_x$ superlattice undulator crystal with period length of 9.9 μm produced at the Aarhus University (UAAR). The high quality electron beam with an energy of 375 MeV of the Mainz Microtron MAMI has been employed. We remind the reader on the experiments already performed with this undulator at beam energies of 270 and 855 MeV [10, 11]. A Fourier analysis of the amplitude distribution for the (110) plane of the undulator yields 4.79 Å, see Ref. [11, Fig. 1], from which an undulator parameter $K = 0.223$ and an expected peak energy of the undulator radiation of 0.132 MeV can be deduced.

The experimental setup is shown in Fig. 7. The undulator crystal was mounted on goniometers with which rotations around three axes could be accomplished. Details on the goniometers, the procedure to align the crystal, etc., are described in Ref. [25]. Photon spectra are shown in Fig. 8. The calculated bremsstrahlung contributions, corresponding to the crystal tuned to a random off-channeling position, are shown in panel (a) as light blue and red lines. These contributions have been subtracted in panel (b). Further details of the analyzing procedure

[4] That an increased ″quantum state″ dechanneling length might still be observable at beam energies as large as a few hundred MeV was brought to our attention at a meeting at FIAS [33].

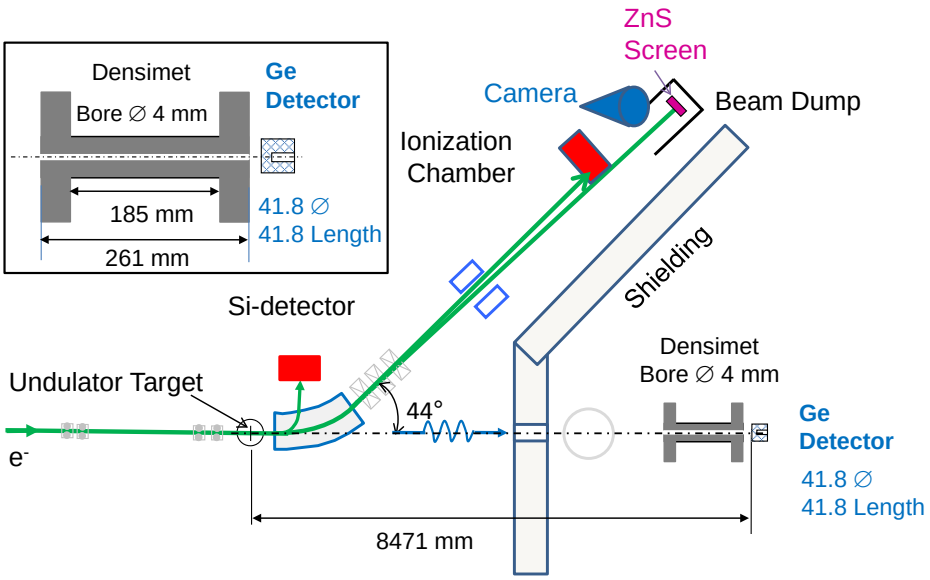

Figure 7. Experimental setup at MAMI. Downstream the undulator target the beam is deflected horizontally by a 44°-bending magnet and thereafter vertically by a second 7.2°-bending magnet. The ionization chamber and the Si detector are monitor counters for the detection of channeling. Photon spectra are recorded with a Ge(i) detector, see inset (bore: 7.8 mm Ø and 30 mm length). The photon beam from the target is collimated with Densimet 176 (density of 17.6 g/cm^3, 92.5% tungsten, 5% nickel, 2.48% iron). The diameters are 52 mm for the inner part and 96 mm for the outer parts. Photons proceed 8.109 m in vacuum and 0.362 m in air just in front of the Ge(i) detector.

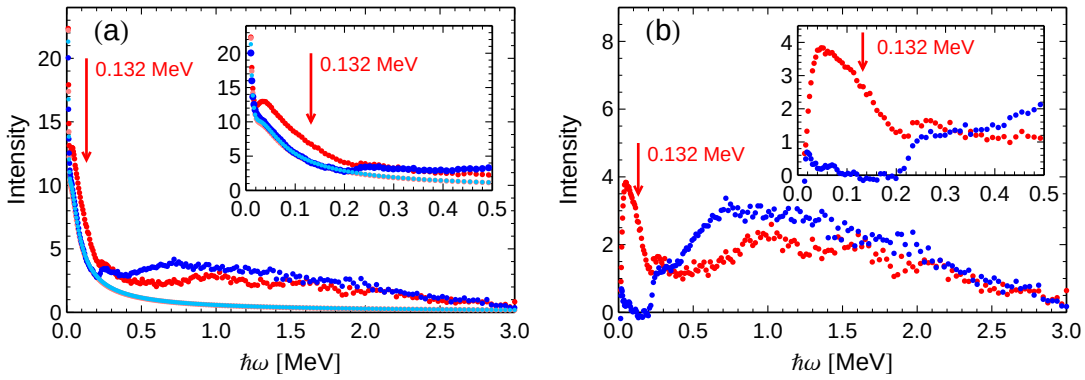

Figure 8. Panel(a): Deconvoluted photon number spectra at (110)-planar channeling of 375 MeV electrons for the flat (blue) and the undulator crystal (red) with effective thicknesses of 49.5 μm and 39.6 μm, respectively. Data were taken with the Ge detector, see Fig. 7. - Panel (b): Same as panel (a) with the bremsstrahlung background subtracted.

are described in Ref. [11].

In the next section we will refer to a model with the aim to understand the origin of the low energy excess yield of the undulator crystal at least qualitatively.

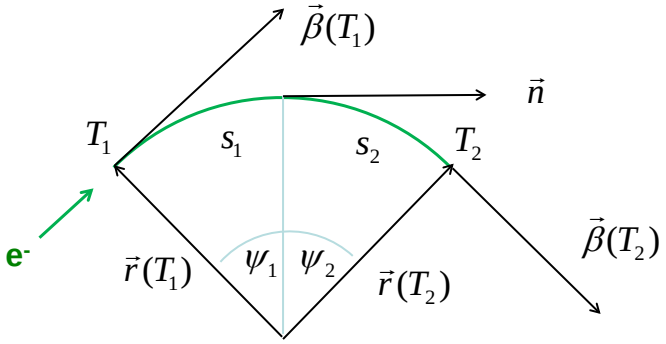

Figure 9. Synchrotron radiation emission from a single finite arc element of the undulator. At times T_1 and T_2 the electron has reduced velocity vectors $\vec{\beta}(T_1)$ and $\vec{\beta}(T_2)$, respectively. For the corresponding radius vectors holds $|\vec{r}(T_1)| = |\vec{r}(T_2)| = \rho$. The vector $\vec{n}$ denotes the observation direction in the plane of the circular arc with bending radius ρ the electron moves.

4. Model calculations

The most striking feature of the spectra shown in Fig. 8 is the enhancement of the radiation intensity for the undulator crystal at low photon energy around 0.1 MeV. We will show that this excess yield is most probably related to synchrotron-like radiation emission.

4.1. Synchrotron-like radiation emission

As has been described in detail in Ref. [11], the undulator consists in a very good approximation of totally eight circular arcs with a bending radius of 6.60 mm. Therefore, we consider synchrotron-like radiation emission as the basic process. On a first glance this picture seems to fail since the critical energy for synchrotron radiation emission $\hbar\omega_c \simeq (3/2)\gamma^3\hbar c/\rho = 17.7$ keV turns out to be much too low. However, the prerequisite for Schwinger's approach with which this formula has been derived, see e.g. Ref. [34, ch. 14.6], is not at all valid for our undulator. We find an arc angle of $\psi_1 = \psi_2 = 0.375$ mrad, see Fig. 9, which is significantly smaller in comparison with $1/\gamma = 1.36$ mrad. This immediately tells that Schwinger's approach with integration from -∞ to +∞ must fail. Because of this fact the emitted time impulse is much shorter and the spectral distribution much broader than calculated with Schwinger's formalism.

The radiation amplitudes from the eight arcs of the undulator must be superimposed coherently taking into account de- and rechanneling. While in a bent crystal strong dechanneling is expected, enhanced by centrifugal forces, at the same time also a significant rechanneling may occur since after half an undulator period all electrons will find a proper direction for rechanneling. This situation is quite dissimilar in comparison with a plane crystal for which the fraction of electrons which scatter back into the nominal direction continuously decreases as function of the traversed crystal depth. It has been assumed in our model that rechanneled electrons again emit a coherent wave train but, of course, without the contribution from the first pole. The corresponding intensity of the second wave train has been added incoherently to the intensity of the first one. This procedure continues until the electron has reached the last pole. Consequently, the irradiated photon number intensity is given by the first term of the formula

$$\frac{d^2N}{d\Omega d\hbar\omega} = \frac{d^2N_S}{d\Omega d\hbar\omega}\sum_{n=1}^{2n_u} p_n |S_n(\hbar\omega)|^2 + \frac{d^2N_W}{d\Omega d\hbar\omega}\sum_{n=1}^{2n_u}(1-p_n) \tag{6}$$

with $d^2N_S/d\Omega d\hbar\omega$ the radiation contribution from a single pole and $S_n(\hbar\omega)$ the structure factor, both described in Ref. [11], n_u the number of undulator periods, and p_n the channeling

probability at pole n. The remaining fraction $(1 - p_n)$ of electrons which does not channel are assumed to produce an incoherent radiation contributions $d^2N_W/d\Omega d\hbar\omega$ at each pole of the undulator. It has been assumed that the electrons emit radiation either by performing a sort of "orbiting" along a crystal channel in a rather tiny fraction of the arc, or in a volume reflection process. In the latter, see, e.g. Ref. [35] and references cited therein, electrons are deflected by the crystal potential without being channelled. We have not estimated whether the corresponding radiation component is of significance for our experiment, or not. In case it would be, one might assume that the orbit in the turning point can be approximated also by a circular arc and, as a consequence, synchrotron-like radiation emission from volume reflection can approximately also be subsumed into the second term of Eqn. (6).

4.2. Description of the fitting procedure

The shape of the radiation spectra depends on several parameters which must be adapted in a fitting procedure. Most sensitively enters the dechanneling length L_d via the structure factor $S_n(\hbar\omega)$ which controls the shape of the undulator peak. The channeling probabilities p_n are described by the recursion relation

$$p_{n+1} = p_n \cdot (1 - p_{de}) + [1 - p_n \cdot (1 - p_{de})] \cdot p_{re}. \tag{7}$$

The p_n depend on the three parameters p_1, p_{de}, and p_{re} which are the initial channeling probability at the first pole, the dechanneling, and rechanneling probabilities, respectively. The rechanneling probability has been assumed to be independent on the pole number what is a rough approximation. The dechanneling probability is assumed to be connected with the dechanneling length by the relation $p_{de} = 1 - \exp[-(\lambda_U/2)/L_d]$. The synchrotron-like radiation intensity for a single undulator pole $d^2N_S/d\Omega d\hbar\omega$ has been calculated for a full arc, and no additional parameter enters. The single incoherent de- or reflection intensity $d^2N_W/d\Omega d\hbar\omega$ depends on an additional parameter ψ_W, assuming $\psi_1 = \psi_2$, see Fig. 9. This parameter controls the intensity and the slope of the spectral component extending to higher photon energies.

The analytical model has totally fife parameters which have been varied by a trial and error method until an acceptable fit of the photon spectra below about 200 keV was achieved. In this region the channeling radiation component for the undulator crystal is assumed to be small, as it is for the plane crystal. Real sensitive are only four parameters, L_d, p_{re}, ψ_W, and the plasma frequency $\hbar\omega_p$. For silicon at random orientation the latter is $\hbar\omega_{p,mean} = 31.06$ eV. However, at channeling it should be somewhat larger because of an enhanced overlap of the electron with an atomic plane where the charge density is larger than in the mean. Indeed, the fit improved significantly by choosing a value 1.2 $\hbar\omega_{p,mean} = 37.27$ eV. It was found that L_d, p_{re} are strongly correlated to each other.

Care has been taken to reproduce the total spectrum which includes the bremsstrahlung contribution. The latter has been calculated for our experimental geometry with well known formulas [36, Eqn. (10.2)] taking into account also the density effect [37, ch. 3] and transition radiation emission. The latter should be absent at on-axis observation as in our experiment. However, scattering of the electron in the target results in a contribution from the rear surface. These contributions are of importance in the low energy part of the spectrum, below about 30 keV. The calculated undulator contribution was added to the calculated bremsstrahlung spectrum and the resulting shape of the sum spectrum was compared with the measured one.

5. Results and discussion

The result of the best fit procedure described in the previous section is depicted in Fig. 10. We find a reasonable good overall agreement with the parameters quoted in the figure caption. The arc length, responsible for emission of the incoherent part, is $L'_d \approx (\psi_W/y'_{max})\lambda_U/2 = 0.99$ μm

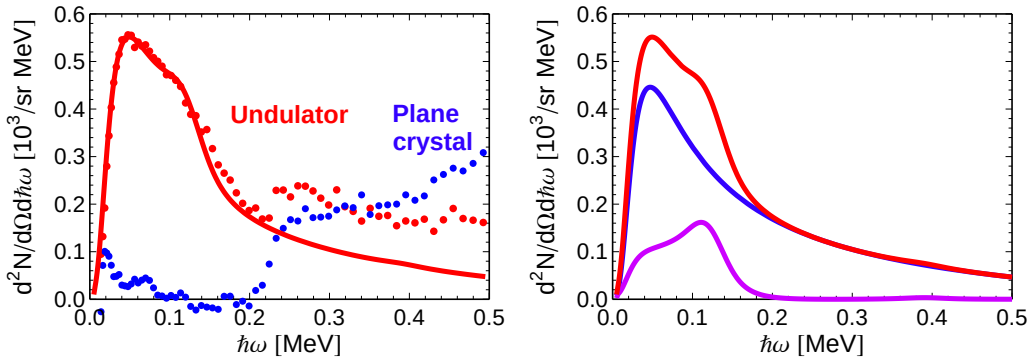

Figure 10. Left panel: Result of the best fit. The data points are taken from Fig. 8 right panel (inset) which were scaled by a factor of 0.145. The full red line represents the calculated undulator radiation line shape for which the following set of parameters were used: $L_d = 4.0$ μm ($p_{de} \approx 0.71$), $\psi_W = 0.075$ mrad, $p_1 = 0.02$, and $p_{re} = 0.01$. The channeling probability drops from 0.02 at the first pole to about 0.014 at the last pole of the undulator. Right panel: Decomposition of the calculated spectrum. The blue spectrum represents the incoherent synchrotron-like radiation contribution, second term of Eqn. (6), the violett the coherent contribution, first term of Eqn. (6). The red curve is the sum of both.

which is rather small. It might be interpreted as dechanneling length of weakly bound electrons in the crystal potential. Whatever the explanation might be, also radiation in the volume reflection process may not be excluded, these rather sharp pulses in the time domain describe already the experimentally observed gross structure quite well, as can be concluded from Fig. 10, right panel (blue curve). It should be mentioned that the deconvolution procedure introduces some systematic errors which could well be in the order of 20 %.

The hump at the expected peak energy of 0.132 MeV can only be reproduced by the coherent term in Eqn. (6) originating from a small fraction of only about 2 % of electrons with a dechanneling length of about 4.0 μm, see Fig. 10, right panel (violet curve). In view of what has been discussed in section 2.3 it might be tempting to speculate that this fraction are electrons which are deeply bound in the crystal potential, i.e. occupying a quantum state.

Let us discuss why the coherence length turns out to be only about 4.0 μm while a larger value of about 15 μm is expected for a plane crystal, see Fig. 6 (b), although with a rather large error bar. We estimated that centrifugal forces diminish the potential barrier from 22.6 eV to 17.6 eV. It is hardly imaginable that by this lowering by only 22 % the dechanneling length of deeply bound electrons will be reduced to such a small value. Another explanation may be found in a break down of the strain by formation of misfit dislocations in the crystal. Finally, if looking to the $Si_{1-x}Ge_x$ crystal structure microscopically, see Fig. 11, still another explanation may be conceivable. In such a view an isolated germanium atom is surrounded by many silicon atoms resulting in a locally perturbed lattice structure. It is quite possible that a plane in which the electron channels looks microscopically bumpy, with the consequence of a locally fluctuating bending radii. In addition, also the transverse potential may be lowered, similar as for thermal vibrations at increasing temperature. Both effects are expected to reduce the dechanneling length.

It should be mentioned that the following alternative explanation for the coherent fraction must be considered as well. During subsequent emission of the short pulses the phase information might not completely be lost resulting in a partial coherence for the second term in Eqn. (6). This possible explanation could not be ruled out during the preparation of this paper, and presently we cannot claim that the observed interference structure originates from quantum

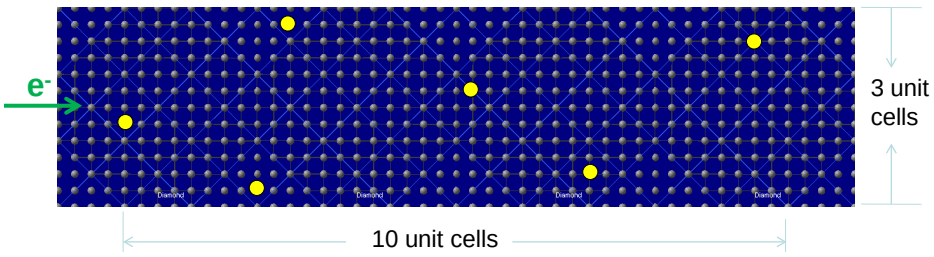

Figure 11. Ge Doping of a silicon single crystal. Shown are $10 \times 3 \times 1$ unit cells with 240 atoms. At 2.5 % doping there are 6 Ge atoms present, i.e. in the mean 0.5 Ge atoms in every of the 12 rows drawn.

state channeling.

In summary, based on a rather simple model with mean trajectories evidence for a weak undulator effect may be concluded also for the experiment at 375 MeV electron beam energy. This finding is in accord with an experiment at 270 MeV [11]. However, there are a number of open questions which might be elucidated by Monte Carlo simulation methods. Various studies are presently underway aiming in a better theoretical understanding of radiation spectra emitted from a crystalline undulator under realistic conditions [38, 39, 40, 42, 43, 41]. In future such simulations may also be of some help for the design of a strong γ-ray source or even a laser on the basis of positrons. At present the reliability of those simulation codes have been or will be tested with the results of our channeling experiments with electrons at MAMI. This fact underlines the importance of the experiments with electrons as described in this paper.

6. Conclusions

Already published dechanneling length measurements [12], employing as signal electrons which have lost about 50 % energy of their primary energy, have been reanalyzed under more realistic model assumptions. The results suggest that low lying quantum states in the channeling potential pocket play an important role. In addition, an experiment with an epitaxially grown strained-layer $Si_{1-x}Ge_x$, 4-period, $\lambda_U = 9.9$ μm undulator has been performed at an electron beam energy of 375 MeV. As for previous experiments at 270 MeV and 855 MeV [11], also in this experiment a clear enhancement of radiation in the expected low energy domain has been observed. Analysis with a simple analytical model suggests that the gross structure can be explained by synchrotron-like radiation emission from small arc elements of the undulator. In order to explain the hump at the expected peak of 0.132 MeV energy, a coherent contribution must be added the origin of which is presently not fully understood. A fraction of about 2 % of the electrons which channel with a dechanneling length of 4.0 μm would explain the experimental observation. Whatever the final explanation will be, the coherent radiation component is rather small. Why this is the case is presently also an open question. Crystal defects may not be excluded. To shed light on this puzzling situation, additional experiment will be analyzed which have been performed at beam energies of 195 and 855 MeV. In addition, experiments have been performed with an undulator for which the Ge content has been reduced by about a factor of two.

Acknowledgments

We gratefully acknowledge fruitful discussions with A.V. Korol, A.V. Solov'yov, and A. Kostyuk, as well as with A. Mazzolari, D. De Salvador, and W. Wagner on experimental details.

This work was supported by the Deutsche Forschungsgemeinschaft DFG under contract BA 1336/2-1.

In part, this work was supported also by the European Commission IRSES CUTE 269131 project (Crystalline Undulator: Theory and Experiment).

References

[1] Kumakhov M A 1976 *Phys. Lett.* **A 57** 17
[2] V.V. Kaplin, S.V. Plotnikov and S.A. Vorob'ev 1980 *Zh. Tekh. Fiz.* **50** 1079-81 [English translation: *Sov. Phys. - Tech. Phys.* **25** 650-51]
[3] Baryshevsky V G, Dubovskaya I Ya and Grubich A O 1980 *Phys. Lett.* **A 77** 61
[4] Korol A V, Solov'yov A V and Greiner W 2004 *Int. J. Mod. Phys.* E **13** 867
[5] Korol A V, Solov'yov A V and Greiner W 2013 *Channeling and Radiation in Periodically Bent Crystals* (Springer Series on Atomic, Optical and Plasma Physics 69)
[6] H. Ikezi, Y. R. Lin-Liu and T. Ohkawa 1984 *Phys. Rev.* **B 30** 1567
[7] Mikkelsen U and Uggerhøj E 2002 *Nucl. Instr. Meth. in Phys. Res.* **A 483** 455
[8] S. C. Jaint and W Hayes 1991 *Semicond. Sci. Technol.* **6** 547-76
[9] Krause W, Korol A V, Solov'yov A V and Greiner W 2002 *Nucl. Instr. Meth. in Phys. Res.* **A 483** 455
[10] Backe H, Krambrich D, Lauth W, Lundsgaard Hansen J and Uggerhøj Ulrik I 2011 *IL NUOVO CIMENTO* **34** C 157-65
[11] Backe H, Krambrich D, Lauth W, Lundsgaard Hansen J and Uggerhøj Ulrik I 2013 Radiation Emission at Channeling of Electrons in a Strained Layer $Si_{1-x}Ge_x$ Undulator Crystal in *Proceedings of the 5th International Conference on Charged and Neutral Particles Channeling Phenomena - Channeling 2012, Alghero, Italy, Sept. 23-28, 2012, Nucl. Instr. and Meth.* **B** in print
[12] W. Lauth, H. Backe, P. Kunz and A. Rueda 2008 *Channeling Experiments with Electrons at the Mainz Microtron MAMI, in Charged and Neutral Particles Channeling Phenomena, Channeling 2008, Proceedings of the 51st Workshop of the INFN ELOISATRON Project, Erice, Italy, 25 October - 1 November 2008, ed. by Sultan B Dabagov & Luigi Palumbo, A. Zichichi* (New Jersey: World Scientific 2010) 335-42.
[13] Beloshitsky V V and Komarov F F 1982 *Phys. Rep.* **93** 117
[14] Andersen J U, Bunderup E and Pantell R H 1983 *Ann. Rev. Nucl. Sci.* **33** 453
[15] Kimball J C and Cue N 1985 *Phys. Rep.* **125** 69
[16] Beloshitsky V V, Komarov F F and Kumakhov M A 1986 *Phys. Rep.* **139** 293
[17] Sáens A W and Überall H 1985 *Topics in Current Physics, Coherent Radiation Sources* (Berlin: Springer)
[18] Carrigan R A and Ellison J A 1987 *Relativistic Channeling, NATO ASI series B: Physics; Vol 165, Proceedings of a NATO Advanced Research Workshop on Relativistic Channeling, Maratea, Italy, March 31 - April 4, 1986* (New York: Plenum Press)
[19] Kumakhov M A and Komarov F F 1989 *Radiation From Charged Particles in Solids* (New York: AIP American Institute of Physics)
[20] Kumakhov M A and Wedell R 1991 *Radiation of Relativistic Light Particles during Interaction with Single Crystals* (Heidelberg, Berlin, New York: Spektrum, Akademischer Verlag)
[21] Berman B L 1991 *Radiation Effects and Defects in Solids* **122-123** 277
[22] Backe H, Lauth W, Rueda A, El-Ghazaly M, Kunz P, Picard A, Scharafutdinov A, Sossalla A and Weber T 2005 *Proceedings of the Memorial Symposium for Gerhard Soff, Frankfurt am Main, Germany, April 25-26, 2005, Topics in Heavy Ion Physics, ed. W. Greiner and J. Reinhardt* (Budapest: EP Systema Bt.) 1-17.
[23] Backe H 2006 *Hyp. Int.* **171** 93-107
[24] Breese M B H 1997 *Nucl. Instr. Meth. in Phys. Res.* B **132** 540-47
[25] Backe H, Lauth W, Kunz P and A. Rueda 2008 *Nucl. Instr. Meth. in Phys. Res.* **B 266** 3835-51
[26] Gouanere M, Sillou D, Spighel M, Cue N, Gaillard M J, Kirsch R G, Poizat J-C, Remillieux J, Berman B L, Catillon P, Roussel L, Temmer M 1988 *Phys. Rev.* **B 38** 4352.
[27] Azadegan B, Wagner W, Pawelke J. 2006 *Phys. Rev.* **B 74** 045209
[28] Kephart J O, Pantell R H, Berman B L, Datz S, Park H and Klein R K 1989 *Phys. Rev.* **B 40** 4249
[29] Komaki K, Ootuka A, Fujimoto F, Horikawa N, Nakanishi T, Gao C Y, Iwata T, Fukui S, Mutou M and Okuno H 1984 *Nucl. Instr. Meth. in Phys. Res.*, **B 2** 71
[30] Adeishvili D I, Bochek G L, Vit'kov V I, Kovalenko G D and Shramenko B I 1985 *Rad. Eff. Lett.* **87** 135
[31] Baier V N, Katkov V M and Strakhovenko V M 1998 *Electromagnetic Processes at High Energies in Oriented Single Crystals* (Singapore, New Jersey, London, Hongkong: World Scientific)
[32] Backe H, Lauth W, Kunz P and Rueda A 2008 *Charged and Neutral Particles Channeling Phenomena, Channeling 2008, Proceedings of the 51st Workshop of the INFN ELOISATRON Project, Erice, Italy 15 October - 1 November 2008, ed. Sultan B Dabagov & Luigi Palumbo, A. Zichichi* (New Jersey: World Scientific) 335-42

[33] Solov'yov A V, Korol A V, Kostyuk A, Greiner W 2008 *"Electron based undulator"*, talk presented at the PECU meeting, January 18, 2008.
[34] Jackson J D 1999 *Classical Electrodynamics, Third Edition* (New York, etc.: John Wiley&Sons, Inc.)
[35] Guidi V. and Bandiera L 2012 *Phys. Rev.* **A 86** 042903
[36] Akhiezer A I, Shulga N F and Truten V I 1998 *Physics Review* Vol **19**
[37] Ter-Mikaelian M L 1972 *High-Energy Electromagnetic Processes in Condensed Media* (New York, London, Sydney, Toronto: Wiley Interscience)
[38] Kostyuk Andriy, Korol Andrei, Solovyov Andrey and Greiner Walter 2011 *J. Phys. B. At. Mo. Opt. Phys.* **44** 075208
[39] Kostyuk A, Korol A V, Solovyov A V and Greiner W 2012 arXiv: 1104.3890v2 [physics.acc-ph]
[40] Kostyuk A 2013 Recent Progress in the Theory of Crystalline Undulator in *Proceedings of the 5th International Conference on Charged and Neutral Particles Channeling Phenomena - Channeling 2012, Alghero, Italy, Sept. 23-28, 2012, Nucl. Instr. and Meth.* **B** in print
[41] Kostyuk A 2013 *Phys. Rev. Lett.* **110** 115503
[42] 2013 Sushko G B, Bezchastnov V G, Solov'yov I A, Korol A V, Greiner W and Solov'yov A V *Simulation of Ultra-Relativistic Electrons and Positrons Channeling in Crystals with MBN Explorer*, Frankfurt Institute of Advanced Studies, Preprint 2013, submitted to Journal of Computational Physics
[43] Baryshevsky V G and Tikhomirov V V 2013 *Crystal Undulators: from the Prediction to the Mature Simulations in Proceedings of the 5th International Conference on Charged and Neutral Particles Channeling Phenomena - Channeling 2012, Alghero, Italy, Sept. 23-28, 2012*, Nucl. Instr. and Meth. B, in print